Application of Surface Impedance Concept to Inverse Problems of Reconstructing Transient Currents

Luca Di Rienzo, Nathan Ida, *Senior Member, IEEE*, and Sergey Yuferev, *Member, IEEE*

***Abstract*—The inverse eddy-current problem of fast transients is solved by a new boundary element formulation employing time domain surface impedance boundary conditions. The integral equation is transformed to invariant form and is solved only once for a given geometry of the problem. Numerical results are in good agreement with measured data.**

***Index Terms*—Boundary element calculations, eddy currents, magnetic sensors, time dependent magnetic fields.**

I. Introduction

In MANY practical problems, such as protection of power systems, measurement of transient currents flowing in massive parallel conductors is required. Traditional low cost current sensors demonstrate poor performance when applied to fast transients. Recently, innovative low cost ac current sensors have been proposed, based on magnetic sensor arrays and digital signal processing techniques [1]. The present paper describes a new algorithm to extend the applicability of those novel sensors to measurement of transients. The proposed technique can be applied when the duration of the current transient is so short that the electromagnetic field has no time to penetrate deep into conductor and remains concentrated near its surface. A natural way in this case is to eliminate the conducting region from the numerical procedure by using the time-domain surface impedance boundary condition (SIBC) at the conductor/dielectric interface. Thus, only the surface of the conductors has to be discretized and the boundary element method (BEM) can be used.

However, direct implementation of time-domain SIBC for the BEM leads to one general shortcoming, namely: the integral equations contain the time convolution product and have to be solved at every time step. This disadvantage, making the method computationally expensive, may be overcome if the total currents flowing in the conductors are correlated in time. Recently, so-called invariant BEM-SIBC formulations allowing for separation of variables into spatial and time components for any time-dependence of the current passage have been developed for conductors of linear materials [2]. The integral equations in the invariant form have to be solved only once for a given system of conductors and then the results for any source field can be easily obtained. In this paper, the invariant formulation is developed for inverse problems of reconstructing transient currents.

II. Statement of the Problem

Consider a system of N parallel conductors of arbitrary cross sections in which transient currents $I_i(t), i = 1, 2, \ldots, N$, flow from an external source. Direct the z axis of the global Cartesian system along the conductors so that the problem can be treated as two dimensional in the xy plane. Parameters of the conductor material and surrounding dielectric space are assumed to be constant. Let M magnetic sensors be located at the positions $\vec{r}_k^{\,\text{sens}}$, $k = 1, 2, \ldots, M$, in the dielectric space separating conductors. A magnetic sensor gives an output voltage signal equal to

$$V_k(t) = S_k \left(\vec{s}_k \cdot \vec{H}\left(\vec{r}_k^{\,\text{sens}}, t\right) \right), \qquad k = 1, \ldots, M \tag{1}$$

where S_k is the sensor sensitivity and $\vec{s}_k$ is the unit vector indicating the sensitivity direction of the sensor. Let the signals be correlated in time so that the following decomposition can be done:

$$V_k(t) = V_k^s T_0(t), \qquad k = 1, \ldots, M \tag{2}$$

where V_k^s, $k = 1, 2, \ldots, M$ are constant coefficients and $T_0(t)$ is a time-dependent function.

Let the time variation of the incident field be such that the penetration depth δ into the body remains small as compared with the characteristic size D of the conductor cross section

$$\delta = \sqrt{\frac{\tau}{(\sigma\mu)}} \ll D \tag{3}$$

where τ is the duration of the incident current pulse and σ and μ are electric conductivity and magnetic permeability of the conductor's material, respectively.

In the inverse problem the output voltage at the location of the sensors is known (measured) and the goal is to calculate the total currents in the conductors.

III. Scalar Potential Formalism

We use the following decomposition of the magnetic field in free space to introduce the magnetic scalar potential ϕ:

$$\vec{H} = \vec{H}^{\text{fil}} - \nabla\phi \tag{4}$$

$$\vec{H}^{\text{fil}} = \sum_{i=1}^{N} \vec{H}_i^{\text{fil}}. \tag{5}$$

Here, $\vec{H}_i^{\text{fil}}$ is the magnetic field created by the current I_i flowing through an assumed filament located at the position

Manuscript received June 18, 2002.

L. Di Rienzo is with the Dipartimento di Elettrotecnica, Politecnico di Milano, 32-20133 Milano, Italy (e-mail: luca.dirienzo@polimi.it).

N. Ida is with the Department of Electrical Engineering, The University of Akron, Akron, OH 44325-3904 USA (e-mail: ida@uakron.edu).

S. Yuferev is with Nokia Mobile Phones, Salo FIN-24101, Finland (e-mail: sergey.yuferev@nokia.com).

Digital Object Identifier 10.1109/TMAG.2003.810197

$\vec{r}_i^{\,\mathrm{fil}}$ inside the conductor [3]. The field $\vec{H}_i^{\mathrm{fil}}$ is obtained from the Biot–Savart law

$$\vec{H}_i^{\mathrm{fil}}(\vec{r},t) = \frac{I_i(t)\left[\vec{e}_z \times \left(\vec{r}-\vec{r}_i^{\,\mathrm{fil}}\right)\right]}{2\pi\left|\vec{r}-\vec{r}_i^{\,\mathrm{fil}}\right|^2}$$

$$\left|\vec{H}_i^{\mathrm{fil}}(\vec{r},t)\right| = \frac{I_i(t)}{2\pi\left|\vec{r}-\vec{r}_i^{\,\mathrm{fil}}\right|} \tag{6}$$

where $\vec{e}_z$ is a unit vector directed along the z axis. Substitution of (4), (5), and (6) into (1) yields

$$V_k(t) = \sum_{i=1}^{N} S_k\alpha_{ki}I_i(t) - S_k\vec{s}_k\cdot\nabla\phi\left(\vec{r}_k^{\,\mathrm{sens}},t\right), \quad m = 1\ldots M \tag{7}$$

$$\alpha_{ki} = \frac{\left(\vec{e}_z \times \left(\vec{r}_k^{\,\mathrm{sens}}-\vec{r}_i^{\,\mathrm{fil}}\right)\right)\cdot\vec{s}_k}{2\pi\left|\vec{r}_k^{\,\mathrm{sens}}-\vec{r}_i^{\,\mathrm{fil}}\right|^2}. \tag{8}$$

Since the scalar potential in free space obeys the Laplace equation, the boundary integral equation method yields the following surface integral equation:

$$c\phi + \sum_{i=1}^{N}\int_{L_i}\phi\frac{\partial G}{\partial\vec{n}}dl = \sum_{i=1}^{N}\int_{L_i}G\frac{\partial\phi}{\partial\vec{n}}dl \tag{9}$$

where L_i is the contour of the cross section of the conductor i, G is the fundamental solution of the two-dimensional (2-D) Laplace equation in free space, and the unit normal vector $\vec{n}$ is chosen inwards. Taking into account (4), (9) can be rewritten in the form

$$c\phi + \sum_{i=1}^{N}\int_{L_i}\phi\frac{\partial G}{\partial\vec{n}}dl = \sum_{i=1}^{N}\int_{L_i}G\vec{n}\cdot\left(\vec{H}^{\mathrm{fil}}-\vec{H}\right)dl. \tag{10}$$

Equation (10) should be supplemented by another relation between the functions ϕ and $\vec{n}\cdot\vec{H}$. The Leontovich surface impedance boundary condition can be used in this role [2]

$$\vec{n}\cdot\vec{H} = (\sigma\mu)^{-1/2}(\pi)^{-1/2}t^{-1/2}\cdot\nabla_s\cdot\vec{H}. \tag{11}$$

The asterisk denotes a time-convolution product and the operator of surface divergence $\nabla_s\cdot$ is defined as follows:

$$\nabla_s\cdot\vec{f} = \nabla\cdot\left[\left(\vec{n}\times\vec{f}\right)\times\vec{n}\right]. \tag{12}$$

Substituting (4) into (11) and (12), we obtain

$$\vec{n}\cdot\vec{H} = (\pi\sigma\mu)^{-1/2}t^{-1/2}\cdot\left(\nabla_s\cdot\vec{H}^{\mathrm{fil}} - \nabla_s^2\phi\right). \tag{13}$$

Substituting (13) into (10) makes the integral equation formulation solvable with respect to ϕ using the following iteration procedure.

Let $I_i^{(m)}$ be the total currents at the step m. Then, $I_i^{(m+1)}$ are obtained in the following way:

1) calculate $\vec{H}^{\mathrm{fil}}$ using (5)–(6);
2) solve (10) and (13) to obtain $\phi^{(m+1)} = \phi^{(m+1)}(\vec{r},t)$;
3) calculate $\phi_k^{(m+1)}$, $k = 1\ldots M$, in the vicinity of the sensor k by moving the observation point in (10);
4) calculate $\nabla\phi^{(m+1)}$ at the location of each sensor;
5) calculate $I_i^{(m+1)}$ using (7).

When the number of sensors is higher than the number of conductors, Step 5 is performed using the "least squares" algorithm, and a reduction of uncertainty in current reconstruction is obtained.

The procedure described has to be performed at every time step. This disadvantage may be avoided representing the formulation in invariant form [2].

IV. Integral Equation Formulation in Invariant Form

A. Nondimensional Variables

Let us switch to the local orthogonal Cartesian coordinate system (ξ_1,ξ_2,η) defined as

$$\vec{e}_{\xi_1}\times\vec{e}_{\xi_2} = \vec{e}_\eta = \vec{n}; \qquad \vec{e}_{\xi_1} = \vec{e}_z \tag{14}$$

where $\vec{e}_{\xi_1}$, $\vec{e}_{\xi_2}$, $\vec{e}_\eta$ are the unit basis vectors. The characteristic lengths associated with the variables ξ_1, ξ_2, and η are D^* and δ, respectively. We introduce the basic scale factors I^*, D^*, τ^* and S^* (nominal sensitivity of the sensors) for the current, surface coordinates ξ_1, ξ_2, time and sensor sensitivity, respectively. The scale factors for other values can be expressed in terms of the basic scale factors [2]

$$\left.\begin{array}{c} H^* = \frac{I^*}{(4\pi D^*)};\ \phi^* = \frac{I^*}{(4\pi)};\ V^* = \frac{S^*I^*}{4\pi D^*} \\ \eta^* = \delta = \left(\frac{\delta}{D^*}\right)D^* = pD^*;\ \ p = \left(\frac{\tau^*}{(\sigma\mu D^{*2})}\right)^{1/2} \ll 1 \end{array}\right\}. \tag{15}$$

Here, p is a small parameter proportional to the ratio of the skin depth and characteristic size of the conductor cross section.

With nondimensional variables the small parameter p appears in the SIBC (13)

$$\vec{n}\cdot\tilde{\vec{H}} = p\left(\pi\tilde{t}\right)^{-1/2}\cdot\left(\tilde{\nabla}_s\cdot\tilde{\vec{H}}^{\mathrm{fil}} - \tilde{\nabla}_s^2\tilde{\phi}\right)$$

$$\tilde{\nabla}_s\cdot\tilde{\vec{H}}^{\mathrm{fil}} = \sum_{k=1}^{2}\frac{\partial\tilde{H}_{\xi_k}^{\mathrm{fil}}}{\partial\tilde{\xi}_k}; \quad \tilde{\nabla}_s^2\tilde{\phi} = \sum_{k=1}^{2}\frac{\partial^2\tilde{\phi}}{\partial\tilde{\xi}_k^2}. \tag{16}$$

The sign "$\sim$" denotes nondimensional variables.

With the dimensionless variables, (6), (7), and (10) take the form of

$$\left|\tilde{\vec{H}}^{\mathrm{fil}}(\vec{r},t)\right| = 2\sum_{i=1}^{N}\frac{\tilde{I}_i(t)}{\left|\tilde{\vec{r}}-\tilde{\vec{r}}_i\right|} \tag{17}$$

$$\tilde{V}_k(t) = \sum_{i=1}^{N}\tilde{S}_k\tilde{\alpha}_{ki}\tilde{I}_i - \tilde{S}_k\vec{s}_k\cdot\tilde{\nabla}\tilde{\phi}, \ \ k = 1\ldots M \tag{18}$$

$$\frac{\tilde{\phi}}{2} + \sum_{i=1}^{N}\int_{S_i}\frac{\tilde{\phi}\partial G}{\partial\vec{n}}d\tilde{s} = \sum_{i=1}^{N}\int_{S_i}G\left[\vec{n}\cdot\tilde{\vec{H}}^{\mathrm{fil}} - p\left(\pi\tilde{t}\right)^{-1/2}\cdot\left(\tilde{\nabla}_s\cdot\tilde{\vec{H}}^{\mathrm{fil}} - \tilde{\nabla}_s^2\tilde{\phi}\right)\right]d\tilde{s}. \tag{19}$$

Here, $\tilde{\alpha}_{ki} = 4\pi D^*\alpha_{ki}$.

B. Expansions in the Small Parameter

We represent the unknown functions, i.e., $\tilde{\phi}$ and $\tilde{I}_i$, in the form of the power series in the small parameter p

$$\tilde{\phi} = \sum_{k=0}^{\infty} p^k \tilde{\phi}_k; \qquad \tilde{I}_i = \sum_{k=0}^{\infty} p^k \tilde{I}_{ik}. \tag{20}$$

Substituting the expansions (20) into the formulation (17)–(19) and equating the coefficients of equal powers of p, the integral equations for the first and second coefficients of expansions are obtained

$k = 0:$

$$\frac{\tilde{\phi}_0}{2} + \sum_{i=1}^{N} \int_{S_i} \tilde{\phi}_0 \frac{\partial G}{\partial \vec{n}} d\tilde{s} = \sum_{i=1}^{N} \int_{S_i} G \vec{n} \cdot \tilde{\vec{H}}_0^{\text{fil}} d\tilde{s} \tag{21a}$$

$$\tilde{V}_k(t) = \sum_{i=1}^{N} \tilde{S}_k \tilde{\alpha}_{ki} \tilde{I}_{0i} - \tilde{S}_k \vec{s}_k \cdot \tilde{\nabla} \tilde{\phi}_0, \quad k = 1, \ldots, M \tag{21b}$$

$$\left| \tilde{\vec{H}}_0^{\text{fil}}(\vec{r}, t) \right| = 2 \sum_{i=1}^{N} \frac{\tilde{I}_{0i}(t)}{\left| \tilde{\vec{r}} - \tilde{\vec{r}}_i \right|} \tag{21c}$$

$k = 1:$

$$\frac{\tilde{\phi}_1}{2} + \sum_{i=1}^{N} \int_{S_i} \tilde{\phi}_1 \frac{\partial G}{\partial \vec{n}} d\tilde{s} = \sum_{i=1}^{N} \int_{S_i} G \left\{ \vec{n} \cdot \tilde{\vec{H}}_1^{\text{fil}} - \frac{1}{\sqrt{\pi \tilde{t}}} * \left(\tilde{\nabla}_s \cdot \tilde{\vec{H}}_0^{\text{fil}} - \tilde{\nabla}_s^2 \tilde{\phi}_0 \right) \right\} d\tilde{s} \tag{22a}$$

$$0 = \sum_{i=1}^{N} \tilde{S}_k \tilde{\alpha}_{ki} \tilde{I}_{1i} - \tilde{S}_k \vec{s}_k \cdot \tilde{\nabla} \tilde{\phi}_1, \quad k = 1 \ldots M \tag{22b}$$

$$\left| \tilde{\vec{H}}_1^{\text{fil}}(\vec{r}, t) \right| = 2 \sum_{i=1}^{N} \frac{\tilde{I}_{1i}(t)}{\left| \tilde{\vec{r}} - \tilde{\vec{r}}_i \right|}. \tag{22c}$$

C. Separation of Variables

We introduce nondimensional time-dependent function $\tilde{T}_1$

$$\tilde{T}_1 = (\pi)^{-1/2} \tilde{t}^{-1/2} * \tilde{T}_0. \tag{23}$$

We represent $\tilde{\phi}_0$, $\tilde{\phi}_1$, $\tilde{I}_{0i}$, $\tilde{I}_{1i}$, $\tilde{\vec{H}}_0^{\text{fil}}$ and $\tilde{\vec{H}}_1^{\text{fil}}$ in the form

$$\tilde{\phi}_0\left(\tilde{\vec{r}}, t\right) = \tilde{\varphi}_0\left(\tilde{\vec{r}}\right) \tilde{T}_0(t); \quad \tilde{\phi}_1\left(\tilde{\vec{r}}, t\right) = \tilde{\varphi}_1\left(\tilde{\vec{r}}\right) \tilde{T}_1(t) \tag{24}$$

$$\tilde{I}_{0i}(t) = \tilde{I}_{0i}^s \tilde{T}_0(t); \quad \tilde{I}_{1i}(t) = \tilde{I}_{1i}^s \tilde{T}_1(t) \tag{25}$$

$$\tilde{\vec{H}}_0^{\text{fil}}\left(\tilde{\vec{r}}, t\right) = \tilde{T}_0(t) \tilde{\vec{H}}_0^{s\text{–fil}}\left(\tilde{\vec{r}}\right); \quad \tilde{\vec{H}}_1^{\text{fil}}\left(\tilde{\vec{r}}, t\right) = \tilde{T}_1(t) \tilde{\vec{H}}_1^{s\text{–fil}}\left(\tilde{\vec{r}}\right). \tag{26}$$

Then the following transformation can be done:

$$\frac{1}{\sqrt{\pi \tilde{t}}} \cdot \left(\tilde{\nabla}_s \cdot \tilde{\vec{H}}_0^{\text{fil}} - \tilde{\nabla}_s^2 \tilde{\phi}_0 \right) = \tilde{T}_1 \left(\tilde{\nabla}_s \cdot \tilde{\vec{H}}_0^{s-\text{fil}} - \tilde{\nabla}_s^2 \tilde{\varphi}_0 \right). \tag{27}$$

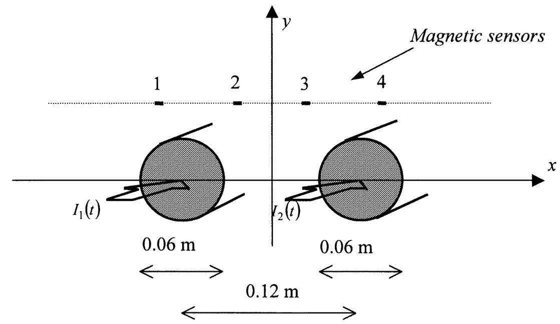

Fig. 1. Experimental setup. Sensors are in positions $x_1 = -0.073$ m, $x_2 = -0.025$ m, $x_3 = 0.023$ m, $x_4 = 0.073$ m; $y_1 = 0.054$ m, $y_2 = 0.054$ m, $y_3 = 0.054$ m, $y_4 = 0.055$ m.

Substituting (23)–(27) into (21) and (22) and taking into account (3) and (19), we obtain the formulations for the spatial functions, as shown in

$k = 0:$

$$\frac{\tilde{\varphi}_0}{2} + \sum_{i=1}^{N} \int_{S_i} \tilde{\varphi}_0 \frac{\partial G}{\partial \vec{n}} d\tilde{s} = \sum_{i=1}^{N} \int_{S_i} G \vec{n} \cdot \tilde{\vec{H}}_0^{s-\text{fil}} d\tilde{s} \tag{28a}$$

$$\tilde{V}_k^s = \sum_{i=1}^{N} \tilde{S}_k \tilde{\alpha}_{ki} \tilde{I}_{0i}^s - \tilde{S}_k \vec{s}_k \cdot \tilde{\nabla} \tilde{\varphi}_0, \quad k = 1, \ldots, M \tag{28b}$$

$$\left| \tilde{\vec{H}}_0^{s-\text{fil}}(\vec{r}) \right| = 2 \sum_{i=1}^{N} \frac{\tilde{I}_{0i}}{\left| \tilde{\vec{r}} - \tilde{\vec{r}}_i \right|} \tag{28c}$$

$k = 1:$

$$\frac{\tilde{\varphi}_1}{2} + \sum_{i=1}^{N} \int_{S_i} \tilde{\varphi}_1 \frac{\partial G}{\partial \vec{n}} d\tilde{s} = \sum_{i=1}^{N} \int_{S_i} G \left\{ \vec{n} \cdot \tilde{\vec{H}}_1^{s\text{–fil}} - \left(\tilde{\nabla}_s \cdot \tilde{\vec{H}}_0^{s-\text{fil}} - \tilde{\nabla}_s^2 \tilde{\varphi}_0 \right) \right\} d\tilde{s} \tag{29a}$$

$$0 = \sum_{i=1}^{N} \tilde{S}_k \tilde{\alpha}_{ki} \tilde{I}_{1i}^s - \tilde{S}_k \vec{s}_k \cdot \tilde{\nabla} \tilde{\varphi}_1, \quad k = 1 \ldots M \tag{29b}$$

$$\left| \tilde{\vec{H}}_1^{s-\text{fil}}(\vec{r}) \right| = 2 \sum_{i=1}^{N} \frac{\tilde{I}_{1i}}{\left| \tilde{\vec{r}} - \tilde{\vec{r}}_i \right|}. \tag{29c}$$

The problems in (28) and (29) can be solved using the iteration procedure described in Section III. Finally, returning to dimensional variables we obtain

$$I = \left\{ \tilde{I}_0^s \tilde{T}_0 + p \tilde{I}_1^s \tilde{T}_1 \right\} I^*; \quad \phi = \left\{ \tilde{\varphi}_0 \tilde{T}_0 + p \tilde{\varphi}_1 \tilde{T}_1 \right\} \frac{I^*}{4\pi}. \tag{30}$$

Formulations enforcing SIBCs of higher orders of approximation can be developed in the same way. Limits of applicability of the approach are discussed in [4].

V. Numerical and Experimental Results

The numerical results obtained using (28)–(30) are compared with data measured by the experimental setup shown in Fig. 1; a pair of identical parallel aluminum conductors of circular cross section are connected in series by a wire and the circuit is fed

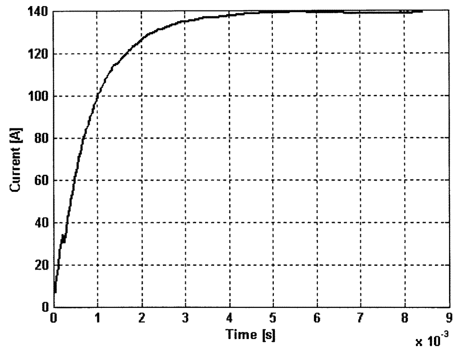

Fig. 2. Transient current waveform.

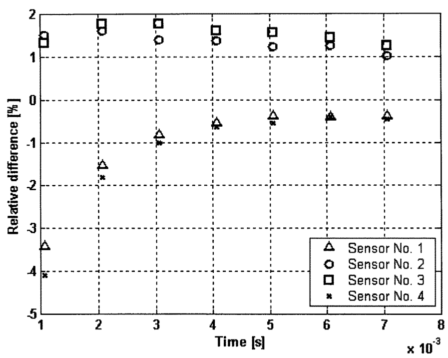

Fig. 3. Relative difference between measured and FEM calculated magnetic fields.

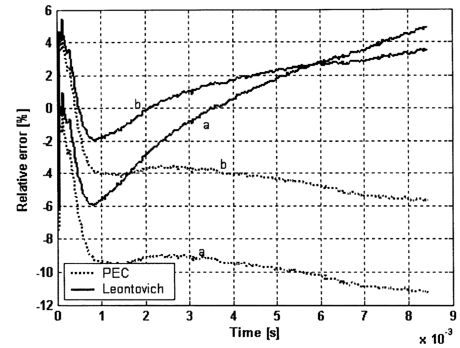

Fig. 4. Relative error of current reconstruction when: (a) two sensors (no. 1 and no. 4) were used and (b) all four sensors were used.

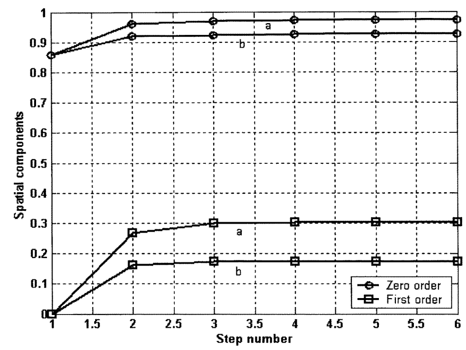

Fig. 5. Spatial components $\tilde{I}_0^s$ and $\tilde{I}_1^s$ versus number of iterations: (a) two sensors (no. 1 and no. 4) were used and (b) all four sensors were used.

by a dc battery so that currents are opposite directed ($I_1(t) = -I_2(t)$). The transient is obtained closing a switch so that the current waveform is exponential, as shown in Fig. 2. Reference current measurement is performed by a commercial close loop Hall effect current transducer whose standard uncertainty is estimated 0.4 A. Four magnetoresistive sensors (Philips KMZ10A) of nominal sensitivity $S = 16$ (mV/V)/(kA/m) are placed as depicted in Fig. 1. Among the main sources of uncertainty in magnetic field measurements one has to consider dc offset both in measurement and in sensors calibration, disturbances due to external magnetic fields and geometrical positions of sensors. Since quantification of the overall measurement uncertainty would be complex and out of the scope of the present paper, the experimental measurements are validated by comparison with a commercial FEM software and relative difference between measured and calculated fields are reported in Fig. 3 at some instants of time.

Fig. 4 shows the relative difference between measured and reconstructed current. The computations are performed in the PEC limit and using the Leontovich SIBC. Note that both formulations are divergent from the actual solution when the steady state is reached and they lose their vailidity.

Two and four sensors have been employed and, as it could be expected, the use of larger number of sensors improves the accuracy in reconstruction. Errors in the Leontovich approximation are of the same order of magnitude of those expected in magnetic field measurements. The technique is then proved to fulfill specifications of current transducers for protection applications, preserving the low cost of the measurement system thanks to the very common magnetic sensors employed. Fig. 5 demonstrates the convergence properties of the proposed iteration procedure.

VI. CONCLUSION

The inverse problem of calculation of the transient currents flowing in the conductors using measured voltages as input is considered. The boundary integral equation formulation employing time-domain surface impedance boundary condition is developed and solved by the iteration procedure. The formulation is transformed to the invariant form admitting separation of variables in space and time components. Thus, the integral equations for a given system of conductors have to be solved only once for any time dependence of the current passage. Numerical results are in good agreement with experimental data.

REFERENCES

[1] G. D'Antona, L. Di Rienzo, A. Manara, and R. Ottoboni, "Processing magnetic sensor array data for AC current measurement in multiconductor systems," *IEEE Trans. Instrum. Meas.*, vol. 50, pp. 1289–1295, Oct. 2000.

[2] S. Yuferev, N. Ida, and L. Kettunen, "Invariant BEM-SIBC formulations for time- and frequency domain eddy current problems," *IEEE Trans. Magn.*, vol. 36, pp. 852–855, July 2000.

[3] I. D. Mayergoyz, "A new approach to the calculation of three-dimensional skin effect problems," *IEEE Trans. Magn.*, vol. 19, pp. 2198–2200, Sept. 1983.

[4] S. Yuferev and N. Ida, "Selection of the surface impedance boundary condition for a given problem," *IEEE Trans. Magn.*, vol. 35, pp. 1486–1489, May 1999.